Enhancement of compression and compaction properties of calcium carbonate powder by granulation with HPC, HPMC and sodium-alginate as binders for pharmaceutical applications: an optimization case study.

Deeb Abu Fara[a*], Iyad Rashid[b], Linda Hmoud[a], Shatha al-Qatamin[c], Babur Z. Chowdhry[d], Adnan A. Badwan[b]

[a]Chemical Engineering Department, School of Engineering, University of Jordan, Amman 11942, Jordan
[b]Research and Innovation Centre, The Jordanian Pharmaceutical Manufacturing Company (JPM), Naor 11710, Jordan
[c]Faculty of Pharmacy and Medical Sciences, Al-Ahliyya Amman University, Jordan
[d]School of Science, Faculty of Engineering & Science, University of Greenwich, Medway Campus, Chatham Maritime, Kent, UK

Received: March 24, 2020; *Accepted:* May 29, 2020

Original Article

ABSTRACT

Calcium carbonate must be processed before it can be compressed into tablets. This study examined the compression behavior of calcium carbonate powder when granulated with different binders. Hydroxypropyl cellulose (HPC), hydroxypropyl methylcellulose (HPMC) and sodium alginate (Na-Alg), were chosen at different concentrations as binding agents. Data analysis and optimization were carried out using load-displacement curves and the Kawakita model of powder compression. The viscosity of the binder solutions, the specific surface area of the granulated $CaCO_3$ and the contact angle of the binder solutions on $CaCO_3$ compact surfaces were used to interpret granulation behavior. Each binder interacted differently with $CaCO_3$ with respect to powder and tablet properties. Optimum tablet processing was found to be strongly dependent on the compression pressure and concentration of the binder used. A 3% binder concentration gave the most desirable outcomes with respect to the area under the load-displacement curves (AUCs), the Kawakita parameter (P_k) and tablet crushing strength (TCS). Calcium carbonate tablets prepared at the optimum binder concentration were stable when stored under accelerated stability conditions.

KEY WORDS: Excipients, binders, calcium carbonate, compactibility, compressibility, direct compression, flowability, load-displacement curve, Gamlen tablet press, granulation, tableting, tablet crushing strength

INTRODUCTION

Calcium carbonate ($CaCO_3$) is one of the most abundant minerals in the earth's crust. It forms various types of rocks such as chalk and limestone. In the oceans, it represents 10% of chemical sediments. Almost all the $CaCO_3$ that makes up the earth's crust is derived from marine organisms, skeletal remains, and other biological constituents that include fecal pellets, lime mud (skeletal), and microbially mediated cement (1). $CaCO_3$ can also be synthesized industrially using different routes of syntheses. The most common routes are via solid-liquid or gas-solid–liquid carbonation (2). These techniques consist of bubbling gaseous CO_2 through concentrated calcium hydroxide, $Ca(OH)_2$, and/or a calcium magnesium hydroxide ($CaMg(OH)_2$) slurry. The large-scale production of $CaCO_3$ in such a

*Corresponding address: Deeb Abu Fara, Chemical Engineering Department, School of Engineering, University of Jordan, Amman 11942, Jordan,
Tel: +962-799182424, E-Mail: abufara@ju.edu.jo

manner contributes to the high cost of the raw material (2, 3).

Both the natural and synthetic forms of $CaCO_3$ can be used as an excipient or as an active pharmaceutical ingredient (API). As the latter, $CaCO_3$ is used as a therapeutic anti-acid and calcium supplement whereas as the former it is used as a filler or diluent (4, 5). In both pharmaceutical uses a high mass content of calcium carbonate must be used in solid dosage forms to provide therapeutic or diluent actions, respectively (6-10).

Generally, tablets produced using raw $CaCO_3$, whether obtained from natural or synthetic sources, are fragile and exhibit low tensile strength (11). This is mainly attributed to two inherent properties of $CaCO_3$ namely surface morphology and deformation upon compression. Regarding surface morphology, Mark *et. al.* (12) and Santoso *et al.* (13) attributed more significance to the morphology parameter than porosity when evaluating the bridging density of the $CaCO_3$ particles and the ensuing tensile strength of the compacts formed. The latter property is not preferred from a deformation perspective when plastic deformation predominantly provides more fresh surfaces for bridging than brittle fracture. Consequently, the presence of smooth flat surfaces results in a low specific surface area and the brittle-fracture nature provides a low number of contact points for binding when $CaCO_3$ powder is subjected to compression. To resolve this issue, researcher have focused on improving the surface-to-surface binding affinity of $CaCO_3$ adopting different approaches (14, 15). One such modification involved the nature of the precipitation process that was used to obtain $CaCO_3$ with a high specific surface area. Under controlled precipitation conditions, the specific surface area increases by 70% from its original value thus resulting in a $CaCO_3$ product with tableting properties equivalent to that of microcrystalline cellulose (16).

Traditionally the most common approach adopted for solid dosage form manufacturing is wet granulation that involves the use of binding agents that ensure surface coverage of the mineral. Maltodextrins, sorbitol, mannitol, maltitol, and xylitol are examples of binders used at a total content of 4-25% (w/w) in wet granulation (17-20). These binders have, however, mostly been tested in research applications, as there are to date, very few registered products on the market. For example, calcium carbonate supplements are manufactured by spray granulation using starch/starch 1500 (21) or maltodextrin/acacia systems (22) and used as binders at a mass content of 10% and 5-10% (w/w), respectively. In addition to the binding effects achieved by using these excipients, the presence of a combination of brittle and plastic/elastic materials provide a synergistic effect to improve powder compressibility and tabletability (23-25). However, the concentration of these binders in solid dosage form manufacturing is largely empirical. Gabbott *et. al.* (26) showed that there is an optimum binder concentration which achieves the highest granule strength. In their work, when $CaCO_3$ was granulated with PEG 1500 at concentrations of $\leq$10% w/w and $\geq$16% w/w, the crushing strength tested on a single granule encountered a substantial decrease from its maximum value which lay between 10% and 14%, w/w. This decrease in crushing strength was due to a lower brittle-fracture behavior as measured by load-displacement (26).

Optimum binder concentration is similarly illustrated in the work of Pusapati *et. al.* (27) where $CaCO_3$ was granulated with acacia at 1.8, 2.54, 3.24% w/w. The Kawakita parameter, P_k, which is indicative of the granule strength, was highest at a binder concentration of 1.8% w/w. Above this value, the P_k value underwent a sharp decrease that correlated with poor tableting properties.

$CaCO_3$ for industrial use is generally obtained from synthetic sources which are usually 99% pure. In the present work, a quarry of geologically deposited $CaCO_3$ was selected from 9 screened sites in Jordan. Different samples from the different quarries were analyzed and showed a $CaCO_3$ content of more than 99%. This finding indicated that the $CaCO_3$ from such sources could be suitable for processing into tablets. Moreover, the very low cost of $CaCO_3$ from the local source (of two-orders of magnitude lower than common sources on the market) motivated investigating the granulation

of the naturally occurring $CaCO_3$ at an API content of >90%. Granulation of $CaCO_3$ with 1-5% (w/w) binder concentration was expected to provide a powder suitable for direct compression.

This aim of this research was to modify the properties of the naturally occurring $CaCO_3$, via process optimization into an industrial commodity suitable for direct compression and handling. Hydroxypropyl cellulose (HPC), hydroxypropyl methylcellulose (HPMC) and sodium alginate (Na-Alg) were tested and evaluated for their binding capabilities at different concentrations. These binders have never been tested with $CaCO_3$ at low concentrations (<5%). Load-displacement curves, Kawakita compression analysis, tablet crushing strength, and the physical properties of the binders were used to determine the optimum binder to the $CaCO_3$ ratio.

MATERIALS AND METHODS

Materials

Highly pure calcite comprising 99.95% w/w $CaCO_3$ (PC-20 grade, of particle size; D_{10}=30 μm and D_{90}=120 μm) was purchased from the Petra Carbonate Factory (Al-Jeeza, Jordan). The natural $CaCO_3$ used was analyzed and found to comply with USP pharmaceutical grade requirements (USP31–NF26). Hydroxypropyl cellulose (JF pharm grade; Ashalnd, Inc, Kentucky, USA), with a viscosity (5% solution at 25°C) of 150-400 mPa.s and an MW of 140,000 Da; Hydroxypropyl methylcellulose (hypomellose K750 PH PRM; Ashland, Inc, Kentucky, USA), with a viscosity (2% solution at 20°C) of 562 mPa.s, MW 250,000 Da and Na-Alg (KIMITEX AX-M; KIMICA Corporation, Chuo-ku, Tokyo, Japan) with a viscosity (1% solution at 20°C) of 300-400 mPa.s were used.

Methods

Preparation of the calcium carbonate granules

Three calcium carbonate powder lots, weighing 495, 485, and 475 g respectively were placed in different trays. Solutions of HPC, HPMC, and Na-Alg were made by dissolving 5, 15, and 25 g of each polymer in 125, 225, and 300 mL, respectively, in distilled water. Granulation was carried out by spraying the calcium carbonate powder with the binding solutions using a generic spray bottle equipped with a spraying nozzle. The powder bed was manually stirred to ensure the spreading of the binder on the $CaCO_3$ surface. This process continued until all the binding solution had been incorporated. The granulated powder was placed in a drying oven at 60°C for one hour. The dried granules were sieved through an 850 μm (#22 mesh size) sieve and collected over sieve size 250 μm. Grinding and crushing were avoided to minimize polymer-$CaCO_3$ adhesion perturbation. This process resulted in calculated polymer concentrations of 1, 3, and 5% (w/w) in the granulations. The final weight of each granulation was in the vicinity of 500 g. Granulated lots were stored in tightly capped containers at room temperature for further evaluation.

Experimental design using response surface methodology

Response surface methodology (RSM) was used to undertake a coherent experimental design to assist in the process optimization of $CaCO_3$ granulation and tableting using different binders at different concentrations. The design was carried out using Design-Expert® software version 11. Two factors were chosen as the independent variables (A) Binder concentration (w/w) and (B) Compression load (kg). The two affected responses were considered (R1) Compression work (kg.mm) and (R2) Tablet crushing strength (kN). RSM optimization of the critical attributes was carried out using Central Composite Design software with three levels for each factor. Lower and upper limits of binder concentrations and compression loads were chosen as 1% (w/w) and 5% (w/w) (coded as -1 and +1), and 100 kg and 300 kg (coded as -1 and +1), respectively. Code 0 represents the middle value between lower and higher limits for binder concentration and compression load (i.e., 3% w/w binder concentration and 200 kg compression load). The star point or α (representing the extreme axial run) was evaluated as 1.414 for a two factorial design shown in Equation 1 (28):

$$\alpha = \left[2^{k} \right]^{1/4} \quad \text{Eq. 1}$$

where; k is the number of factors. The values of the two input parameters and the corresponding codes are shown in Table 1. Data analysis, using ANOVA, was carried out to determine the significance of the experimental factors.

Table 1 Experimental design: values of the inputs and corresponding codes

CODE	FACTOR 1 BINDER CONCENTRATION (%)	FACTOR 2 COMPRESSION LOAD (kg)
-1.414	0.4	60
-1	1	100
0	3	200
1	5	300
1.414	7.0	425

Compaction

200 mg of powdered samples of $CaCO_3$ from the original natural source (used as a reference) and from the 1, 3, and 5% w/w granulated dried powder (sieved through 250-850 μm) were weighed and poured into 6 mm diameter dies. The powders were compressed using a Gamlen tablet press (Gamlen Tableting Ltd., Biocity Nottingham, UK). Compression was repeated twice for each sample at different compression loads (100, 200, 300, 400, and 500 kg). The speed of compression was set at 60 mm/min using a 6 mm circular punch. Lubrication was excluded to avoid the influence of lubricants on the compression data. An example of the resultant load-displacement curve (L-D) is presented in Figure 1. The figure denotes an ascending compression curve that ends at the maximum force applied (± 10 kg) followed by a descending elastic recovery curve. The L-D data were transferred to excel sheets for calculating the area under the compression curve (AUC). AUC represents the work (or energy) input during powder compression.

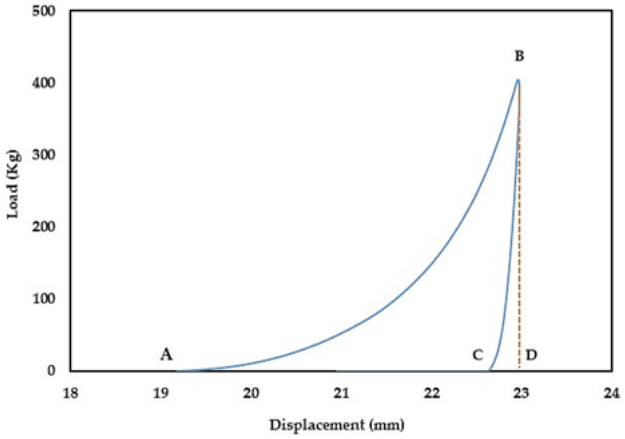

Figure 1 A representative GTP-1 generated load-displacement curve at 400 kg load.

Compression analysis

The Kawakita model was used to analyze compression behavior. This empirical model is predicated on the fact that there is a linear relationship between the [compression pressure/powder volume reduction ratio] and compression pressure shown in Equation 2:

$$\frac{P}{C} = \frac{P}{a} + \frac{1}{ab} \quad \text{Eq. 2}$$

where; C is the degree of volume reduction of the powder column under applied pressure, P. The constant a is the minimum porosity of the material before compression, the constant b relates to the amount of plasticity of the material whereby the reciprocal of b or P_k defines the pressure required to reduce the powder bed by 50% from its initial volume (29, 30).

Crushing strength measurement

Powder compression was investigated using a single punch tablet press (Manesty, County Durham, UK). The use of such a tablet press provides a realistic representation of the actual industrial compression of powders. 200 mg of each of the prepared $CaCO_3$-binder samples was compressed using a 9 mm die. Compression was carried out at forces of 30, 35, 40, 45, and 50 kN. 10 tablets were compressed at each

compression force. The crushing strength of compacts was measured using a crushing strength tester (Copley, Nottm Ltd, Therwil, Switzerland).

Scanning Electron Microscopy (SEM)

A Thermo Fisher Scientific SEM (Eindhoven, Netherlands) was used for the analysis of the samples. Samples of natural $CaCO_3$ and from a 5% w/w granulated dried powder (sieved) were mounted on aluminum stubs and then coated with gold in a low-vacuum sputter coating chamber operating at 1200 V, 20 mA for 105 seconds.

Viscosity measurements

The viscosity of HPC, HPMC, and Na-Alg solutions at concentrations of 1, 3, and 5% w/w were measured using an MCR 302 rotational rheometer with a double gap system (Anton Paar, antonpaar.com). Viscosity was measured when the torque applied was fixed at the lowest plate spindle speed ($0.01 s^{-1}$ shear rate).

Specific surface area (SSA) measurements

The specific surface area measurements (SSA) of the natural and granulated calcium carbonate with HPC, HMPC, and Na-Alg was quantified by gas adsorption using a Sorptomatic 1990 (Carlo Erba Instruments, Rodano, Italy). Samples were initially degassed under vacuum for 24 hours at 70°C, then exposed to nitrogen at 77.4 K (-195.75°C). According to the Brunauer–Emmet–Teller (BET) equation (31, 32), the SSA was determined within a relative pressure range p/p0 between 0.05 and 0.3. Surface areas for each sample were measured in triplicate.

Contact angle measurement

Contact angles of droplets made of HPC, HPMC, and Na-Alg at concentrations of 1, 3, and 5% (w/w) were measured on a $CaCO_3$ compact surface using a contact angle goniometer (DataPhysics, Filderstadt, Germany). Droplets, 500 µL each, were automatically ejected at a dosing rate of 1.0 µL/s through a syringe onto the $CaCO_3$ compact surface. The instrument captured drop images and automatically recorded and analyzed the drop angle via the instrument software which uses a baseline, a curve and a tangent to analyze the droplet image.

Preparation and physical stability of $CaCO_3$ tablets using different binders

Calcium carbonate tablets comprising 90% $CaCO_3$ granulated with either HPMC or Na-Alg were prepared. HPC was excluded in the stability study analysis due to its failure to provide sufficient compressibility and compatibility at the initial compression stage. Two calcium carbonate batches were prepared, each consisting of 3 kg of calcium carbonate granulated with either HPMC or Na-Alg. An aqueous granulating solution containing 110.5 g of each binder was dissolved separately in distilled water in a quantity sufficient to make a clear solution. Calcium Carbonate powder was granulated with the binder solution until a cohesive mass was obtained. The granulated mass was dried in a tray dried oven at 70°C for 3 hours. The dried granulated powder was passed through sieve size (mesh No. 18 equivalent to 1.00 mm opening). Microcrystalline cellulose (215 g), starch sodium glycolate (103 g) sodium lauryl sulfate (15 g), and magnesium stearate (0.1 g) was mixed in a mixer for 7 minutes. Peppermint oil (1.1 g) was sprayed on the powder mixture and mixed for an additional 3 minutes. This mixture was added to the Calcium Carbonate granules in a mixer and mixed for 15 minutes. The granulated mixture was fed to a Manesty single punch tableting machine with a 13 mm punch size and compressed into tablets with a weight of 1440 mg at 45 kN. Each batch produced approximately 2400 tablets. The resulting tablets (with the composition shown in Table 2) were stored in tight containers for further testing.

500 tablets of each batch were stored in open lid bottles in an oven at 40°C at a relative humidity of 75%. Samples were withdrawn initially and at three and six months. At each interval, 100 tablets were withdrawn and were subjected to weight, disintegration, friability,

Table 2 Composition of a single prepared $CaCO_3$ tablet using HPMC or Na-Alg as binders (prepared for physical stability testing)

MATERIAL	% (w/w)	TABLET CONTENT (mg)
$CaCO_3$	86.8	1250
Binder (HPMC, Na-Alg)	3.20	46.02
Microcrystalline cellulose (MCC 101, 50 μm)	6.23	89.70
Sodium starch glycolate (Primojel)	3.00	43.20
Sodium lauryl sulphate (SLS)	0.44	6.32
Peppermint oil	0.03	0.44
Mg stearate	0.30	4.32
TOTAL	100	1440

and hardness testing carried out according to the USP compendia testing method (USP31–NF26- page 1603). Concurrently, the percent water content of the ground tablets was measured using a Karl Fischer volumetric titrator (Mettler Toledo, Hamburg, Germany).

RESULTS AND DISCUSSION

Granulation

The percent v/w of the volume of the granulating liquid to the weight of the $CaCO_3$ was 25%, 46.4%, and 63.2% for binder concentrations (in the subsequently dried granulation) of 1, 3, and 5% respectively. No attempt was made to determine the optimum volume to weight ratio of binder liquid to the mass of $CaCO_3$ (for example using power consumption, thermal effusivity or NIR), thus it was not known if the wet granulation was at the seed formation stage, granule growth stage or over-wetting stage after all the binder solution had been consumed.

Consequently, since the granules that were above 850 microns and below 250 microns were excluded from the tableting analysis, it is possible that the binder concentration in the dried granulation was different from the calculated concentrations of 1, 3, and 5%. Assuming a 10-micron constant thickness volumetric layer on the surface of different sized granules, calculations showed that 77.8% of the calculated binder concentration would be retained in the dry granulation assuming a normal particle size distribution, whereas 82.1% and 66.4% of the calculated binder concentration would be retained in the dry granulation assuming a distribution skewed to the low and the high diameters respectively. This effectively means that experimental binder percent differences of 0.86% could have been compared where the calculated difference would be 2.0% (82.1% of 3% compared against 66.4% of 5%). No attempt was made to determine the particle size distribution of the granules between 250 and 850 microns.

RSM Analysis

Response Surface Method (RSM) was used for the determination of critical attributes of the compression pressure and the binder concentration. A statistical analysis of the quadratic model confirmed that these two factors were statistically significant (Table 3). Coded factors and their set limits (lower to upper) are presented in Table 1. The experimental responses and the 3-dimensional fitted response surface plots

Table 3 ANOVA analysis for the CaCO3-binder systems models

SYSTEM	R1			R2		
		p-Value			*p*-Value	
$CaCO_3$-HPC	**Model**	0.0005	Significant	**Model**	0.0309	Significant
	A-A	0.9933		A-A	0.0243	
	B-B	< 0.0001		B-B	0.0078	
	AB	0.4585		AB	1.00	
	A^2	0.0006		A^2	0.4774	
	B^2	0.5397		B^2	0.1852	
$CaCO_3$-HPMC	**Model**	0.001	Significant	**Model**	0.0005	Significant
	A-A	0.0128		A-A	0.0002	
	B-B	0.0001		B-B	0.0004	
	AB	0.124		AB	0.1889	
	A^2	0.3689		A^2	0.0887	
	B^2	0.0342		B^2	0.0724	
$CaCO_3$-Na-Alg	**Model**	0.0005	Significant	**Model**	0.0192	Significant
	A-A	0.0198		A-A	0.0232	
	B-B	< 0.0001		B-B	0.0052	
	AB	0.300		AB	0.3759	
	A^2	0.0057		A^2	0.6913	
	B^2	0.9147		B^2	0.0847	

obtained are shown in Figure 2. The plots represent the area under the compression curve (compression work) (R1) (kg.mm) and the tablet crushing strength (R2) [N] as a function of binder concentration (A:A) (w/w) and compression load (B:B) (kg).

The RSM results show that when the AUC is considered as the response parameter, the lower (1%) and upper (5%) values of the binder concentration have less effect on the AUCs than medium (3%) values for the HPC binder (Figure 2-A). Furthermore, the highest AUC value was obtained at the highest compression load with 3% HPC. When HPMC was used as a binder, the relationship between its concentration and the AUC values showed a curvilinear relationship but with a shallower "bend" than that obtained with HPC (Figure 2-C). This only occurred at lower values of the compression load. For medium and upper compression load ranges, high AUCs were obtained especially at upper values of binder concentration. The same observation was valid for the tablet crushing strength factor, whereby a sharp increase in crushing strength was found at the upper values of both factors (Figure 2-D). For Na-Alg, RSM analysis showed the same curvilinear relationship between binder concentration and AUC as that for HPC (Figure 2-E). Thus a maximum AUC was obtained at 3% binder concentration up to medium values of the compression load. Furthermore, the AUCs were at a maximum when the compression load exceeded its medium value, and when the binder concentration was minimal. However, the RSM for tablet crushing strength (Figure 2-F), unlike the AUC, showed maximum values at the upper limits of both factors. Moreover, medium values of compression pressure displayed crushing strength values close to the maximum at the 5% binder concentration.

Although the RSM results indicated that maximum crushing strength was obtained at the upper values of both the binder concentration and the compression load (Figure 2-B, D, F), 3% w/w binder concentration, and 300 kg compression load showed comparable crushing strength values. This effect, in terms of the crushing strength, was supported by the RSM finding involving the AUC as well. (Figure 2-A, C, E). The highest AUC value was obtained at the highest compression load of powders granulated with a binder concentration of 3%.

Compression Analysis

Compression analysis of $CaCO_3$ granulated with different binders was performed using the F-D technique. F-D curves were generated using the instrumental tablet press (GTP) for the three different binders at compression loads between 100-500 kg. The area under each curve was numerically calculated and plotted as a function of the binder concentration at each compression load; results are presented in Figures 3, 4, and 5.

For $CaCO_3$ granulated with HPC ($CaCO_3$-HPC), the AUCs at compression loads of 100-400 kg, increased until 3% HPC, and then decreased at 5% w/w HPC (Figure 3). In contrast, when the compression load was increased to 500 kg, the AUC continuously increased with binder concentration. It was also observed that the AUC of granulated $CaCO_3$ was greater than that of the raw material at all binder concentrations and all compression loads (Figure 3).

For $CaCO_3$-HPMC, the AUCs can be divided into two compression regimes; the first one from 100-300 kg, and the second from 400-500 kg (Figure 4). In the lower compression range, the AUCs increased with increasing binder concentration. The previously noted decrease in the AUC for $CaCO_3$-HPC at the 5% w/w level was not detected in this range. However, at higher compression loads of 400 and 500 kg, a decrease in the AUC value upon increasing the binder concentration from 3-5% w/w was, again, evident.

For $CaCO_3$-Na-Alg, the decrease in the AUC at 5% w/w Na-Alg dominated the compression behavior at all compression loads (100-500 kg) (Figure 5). For the 1 and 3% Na-Alg concentration, there was either no change or a statistically insignificant increase in the AUC values. The AUCs of non-granulated natural $CaCO_3$ was lower than that of $CaCO_3$-Na-Alg at all binder concentrations.

The AUC value reflects the extent of deformation,

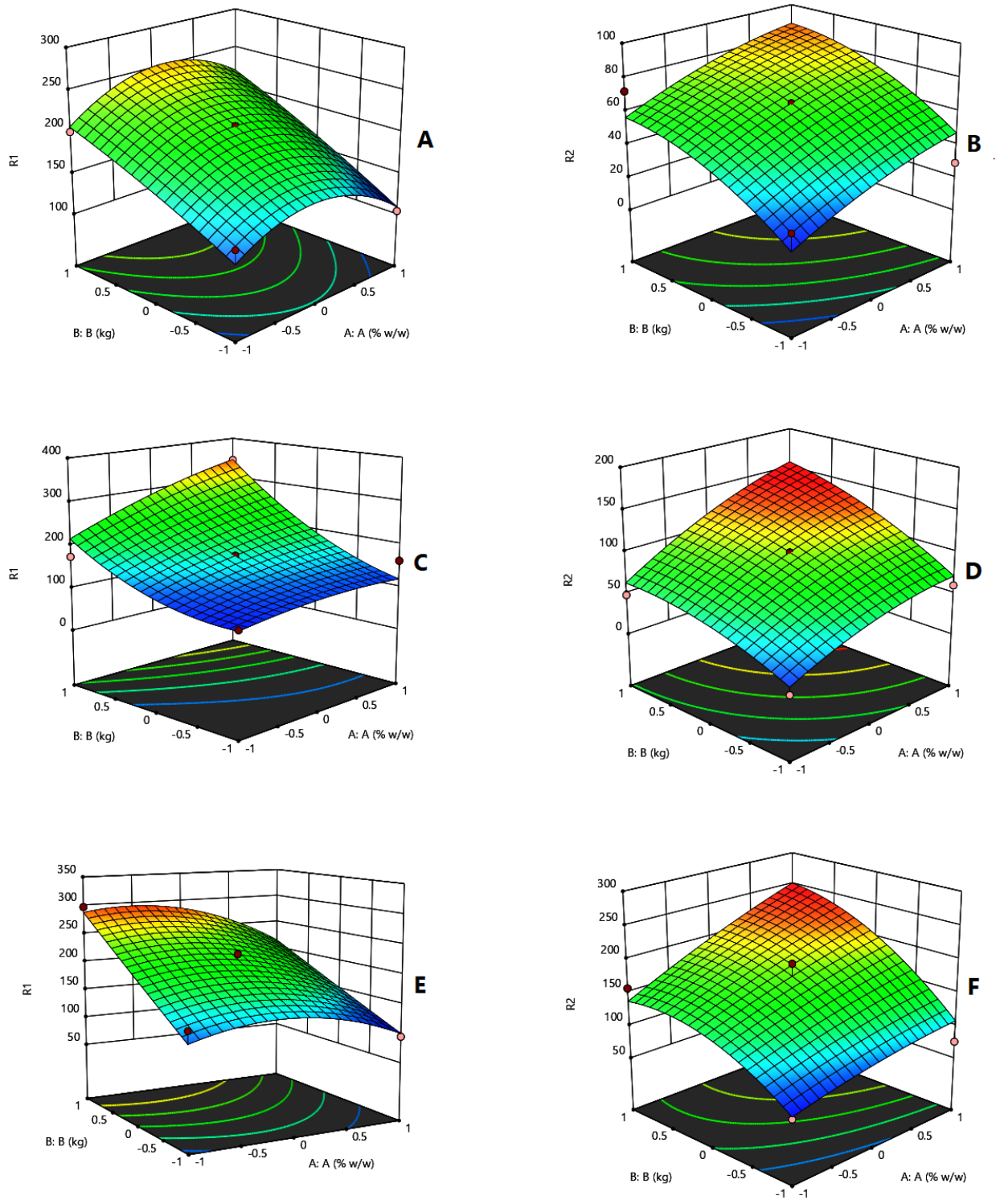

Figure 2 The experimental responses and the 3-dimensional fitted response surface plots for AUC (R1) and tablet crushing strength, TCS (R2) for (A) $CaCO_3$-HPC, (B) $CaCO_3$-HPMC and (C) $CaCO_3$-Na-Alg.

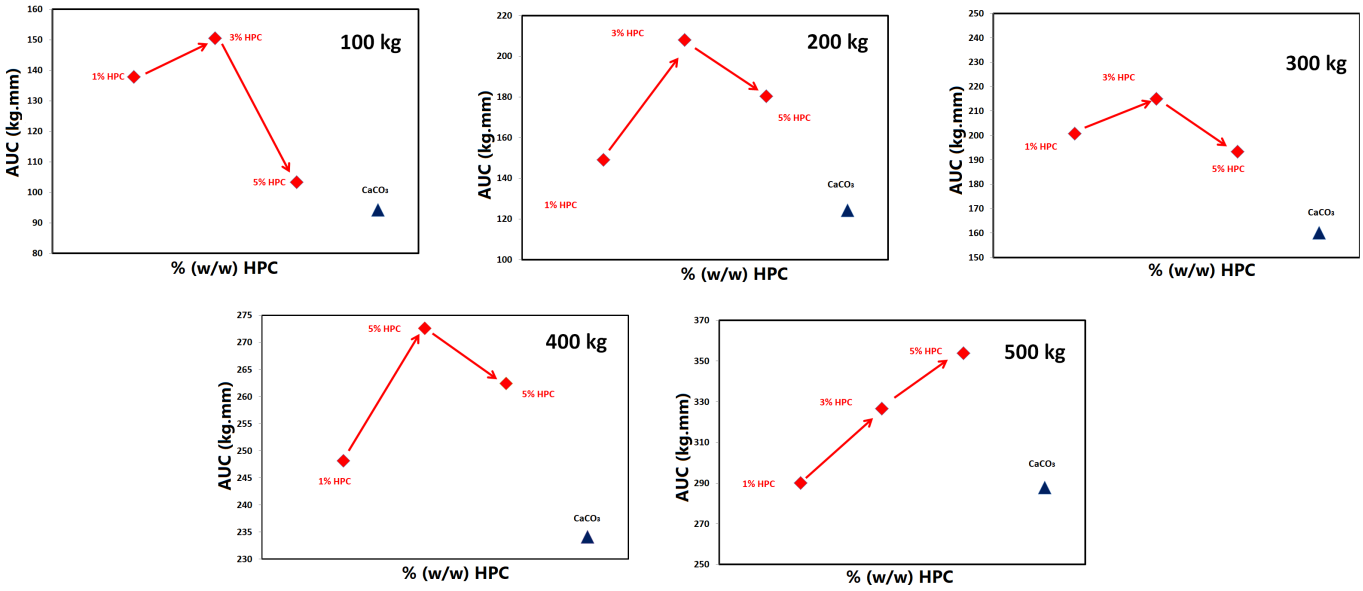

Figure 3 Compression work (AUC) for the $CaCO_3$-HPC system vs. binder concentration at a compression load of 100-500 kg.

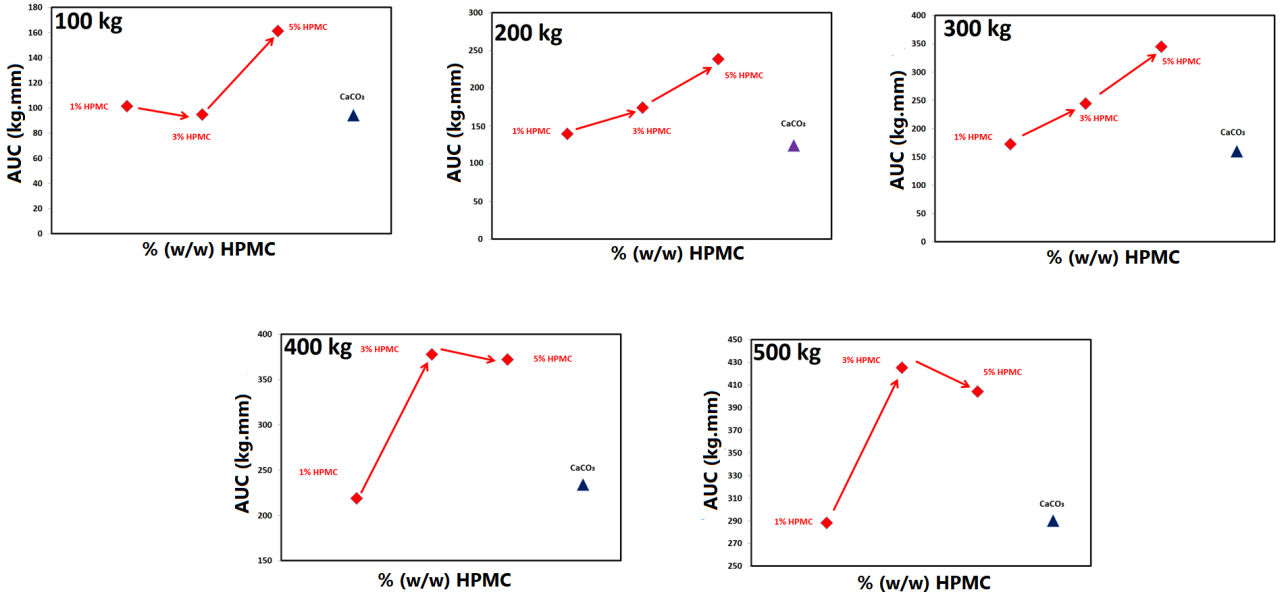

Figure 4 Compression work (AUC) for $CaCO_3$-HPMC system *vs.* binder concentration at a compression load of 100-500 kg.

whether plastic or brittle fracture, taking place upon compression of powders. Such deformation produces new fresh surface-to-surface contacts resulting in hard compacts (30). Thus, it is preferable to optimize powder processing parameters (e.g. compression load) and/or granulation parameters (e.g., binder concentration) so that granules undergo a higher extent of deformation upon compression. For $CaCO_3$ compression, when the extent of fragmentation amongst the granules is high, new fresh surfaces are available for providing more surface contacts, thus resulting in high mechanical strength (32). Hence, high AUC values are desirable to optimize different binder concentrations at different compression loads.

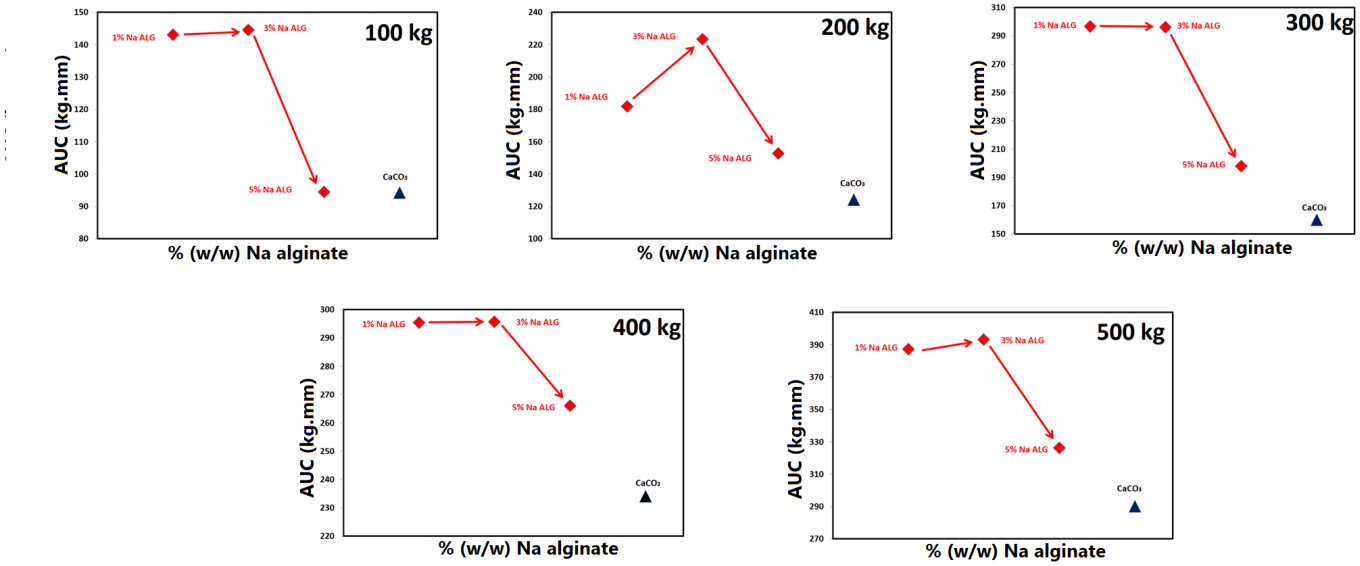

Figure 5 Compression work (AUC) for $CaCO_3$-Na-Alg system vs. binder concentration at a compression load of 100 – 500 kg.

For example, the 5% w/w concentration of HPC in the $CaCO_3$-HPC granules is not optimum concerning AUC values. The 3% w/w concentration of HPC yields a maximum AUC at compression loads between 100-400 kg (Figure 3). At a compression load of 500 kg, the highest AUC value was obtained at 5% HPC. On the other hand, 5% w/w HPMC is more favorable for granulation of $CaCO_3$ at compression loads between 100-300 Kg (Figure 4) whereas 3% HPMC is favorable at compression loads between (400-500 kg; Figure 4), With Na-Alg the maximum AUC occurs the 3% w/w binder concentration over the whole range of compression loads (Figure 5). This implies that Na-Alg, at >3% provides no advantage in maximizing AUC regardless of the compression load used. AUC differences between native $CaCO_3$ and its combination with different binders are greater with HPMC or Na-Alg than with HPC. Hence, the former two binders are able to modify $CaCO_3$ tableting properties better.

The above results obtained from the F-D curve analysis were compared with those obtained by compression analysis using the Kawakita equation. Plots of the P_k values versus the binder concentration are presented in Figure 6. The P_k of un-granulated, raw $CaCO_3$ is included in the data in Figure 6 for comparison. Changes in the P_k values with binder concentration followed a similar trend obtained with the AUC. A maximum P_k was obtained at 3% w/w followed by a decrease at the 5% w/w concentration of each binder.

The similar behavior of changes in *Pk* values to that obtained for most AUC profiles is because both techniques reflect similar properties of powders subjected to deformation upon compression. In other words, the energy of granule deformation (AUC) is equivalent to the load needed for volume reduction (P_k is ½ powder volume reduction). Specifically, the granules with a 3% binder display a greater deformation tendency (as reflected in the greater AUC) than those at 1% or 5%. A high tendency to deformation produces harder granules which consequently require a high compression load to reduce the powder bed volume (high P_k value). In brief, the Kawakita parameter, P_k, produced a 'profile trend' relating to the binder concentration (Figure 6) that matched that of the AUC/binder concentration data at most compression loads investigated (Figures. 3-5). Interestingly, P_k, values calculated for each binder type was based on a linear relationship across the whole compression load range (100-500 kg). This implies that P_k is calculated based upon five compression loads (100-500 kg) whereas each AUC value is based upon one individual compression load. Consequently, the P_k value provides

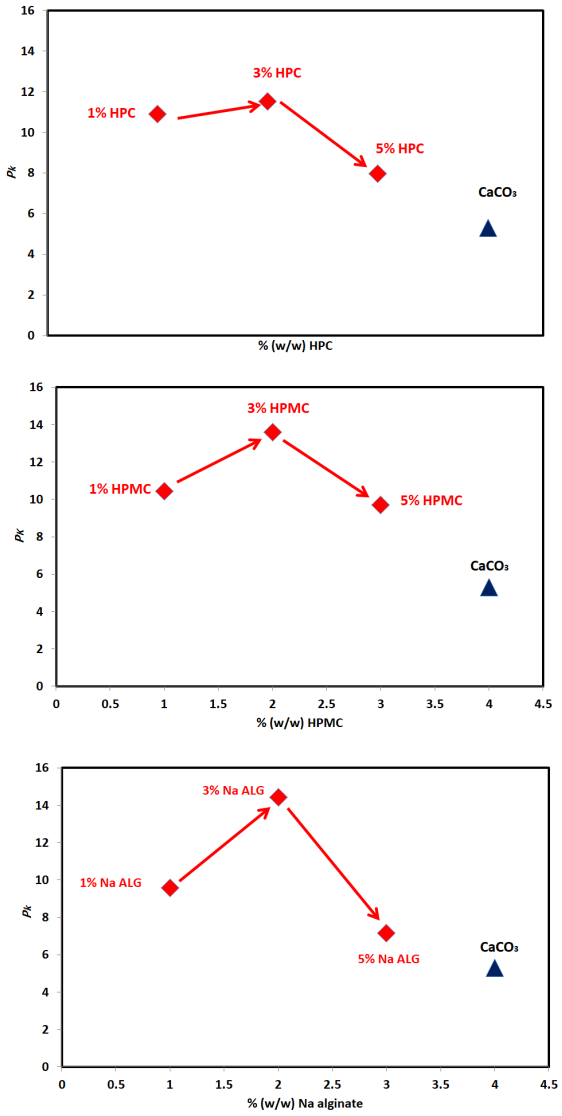

Figure 6 P_k *vs.* binder concentration for the three granulated systems.

an average indication of the granule strength whereas the AUC provides a similar indication but at a specific compression load. Nevertheless, AUC measurements are more specifically informative than P_k values in determining optimum process parameters (such as binder concentration) at each compression load applied. For example, the previously described 'profile trend' was found to deviate at specific compression loads. This was noticed for the data in Figure 3 for HPC at 500 kg and in Figure 4 for HPMC at 100-300 kg wherein the maximum AUCs were obtained at 5% w/w binder. In contrast, the P_k values indicated an optimum binder concentration of 3% (Figure 6).

Crushing strength analysis

Tablet crushing strength is a measure of how efficient the binder is in holding the granules together in a compact with inter- and intra-granular forces. The crushing strength of tablets made of raw $CaCO_3$ and $CaCO_3$ granulated with HPC, HPMC, and Na-Alg, was tested as a function of the compression force at binder concentrations of 1%, 3%, and 5% (w/w). The results are shown in Figure 7.

The crushing strength of tablets made of $CaCO_3$-HPC was not significantly greater than that of the raw $CaCO_3$ tablets at the three binder concentrations tested (Figure 7). The difference was greater at low compression forces up to 35-40 kN, disappearing at higher compression forces.

For $CaCO_3$-HPMC tablets, crushing strength values followed the same behavior as those of $CaCO_3$-HPC tablets whereby there was an increase up to compression forces of 40 kN above which the rate of increase was lesser (Figure 7). The crushing strength profile of raw $CaCO_3$ is included for comparison. Surprisingly, the $CaCO_3$-1% HPMC tablets did not differ from the raw ones with respect to the crushing strength results. It was only at HPMC contents of 3% and 5% (w/w) that the tablets showed marginal differences in crushing strength values compared to the raw ones. Once more, such differences were greater at low compression forces (<40 kN).

The crushing strength values of $CaCO_3$-Na-Alg tablets and their differences compared with natural $CaCO_3$ were the greatest compared to the other two binders at all concentrations of Na-Alg used (Figure 7). The crushing strength of tablets made from these granules showed an initial sharp increase up to 40-45 kN, above which there was either a decline at 1% or no change at 3% and 5%.

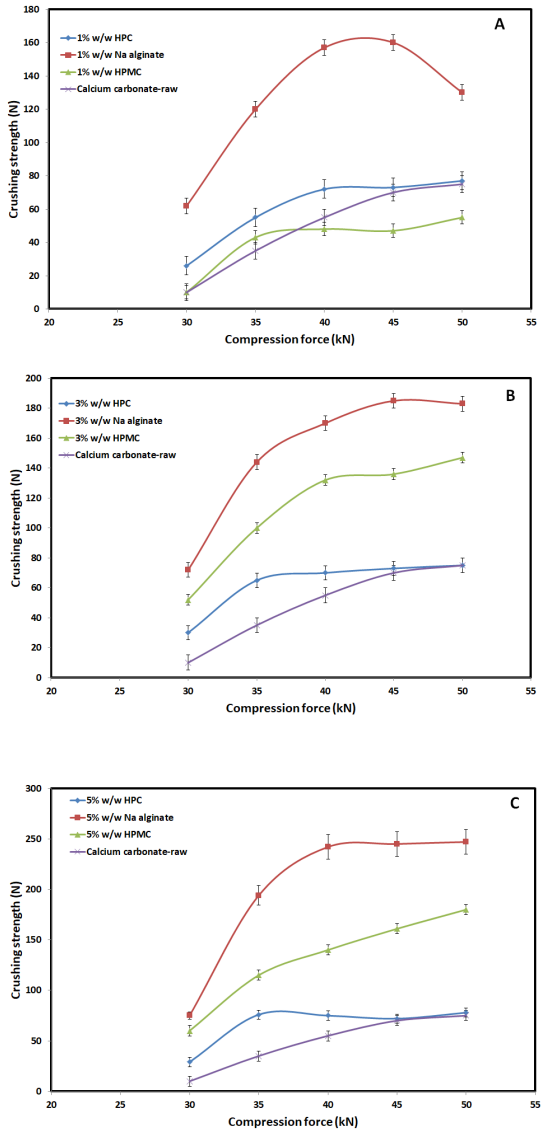

Figure 7 Tablet crushing strength (TCS) *vs.* compression force for $CaCO_3$ powder and granulated $CaCO_3$ with different binders at different concentrations.

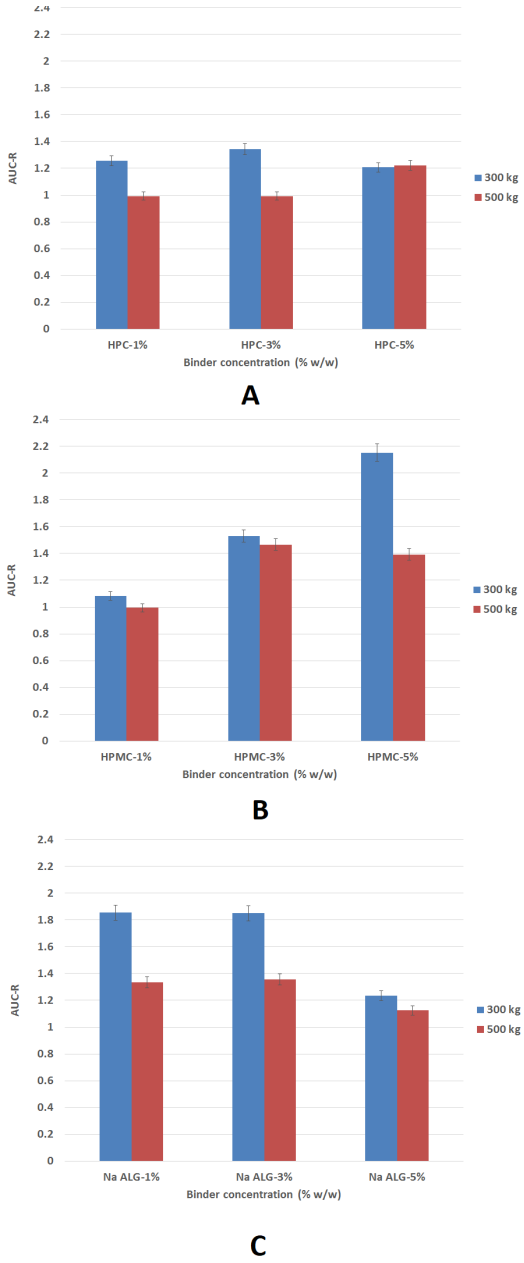

Figure 8 Relative compression work (AUC-R) *vs.* binder concentration for the three granulated systems at 300 and 500 kg compression load

AUC-R and TCS-R ratios

The AUCs and the mechanical strength of tablets consisting of the $CaCO_3$-binder powders at different concentrations of the binders were compared. This was performed using the relative ratios of both parameters, i.e., AUC-R and TCS-R whereby each ratio expresses a quantitative measure of the change of each parameter with respect to the reference. For example, an AUC-R or TCS-R value of <1.0 indicates a lower value of the parameter for granulated $CaCO_3$ than the reference. AUC-R values of each $CaCO_3$-binder sample at 1, 3, and 5% w/w binder concentrations are presented in Figure 8. Compression loads of 300 and 500 kg, representing the low and high values, were used. This was based on the fact that significant changes in AUCs

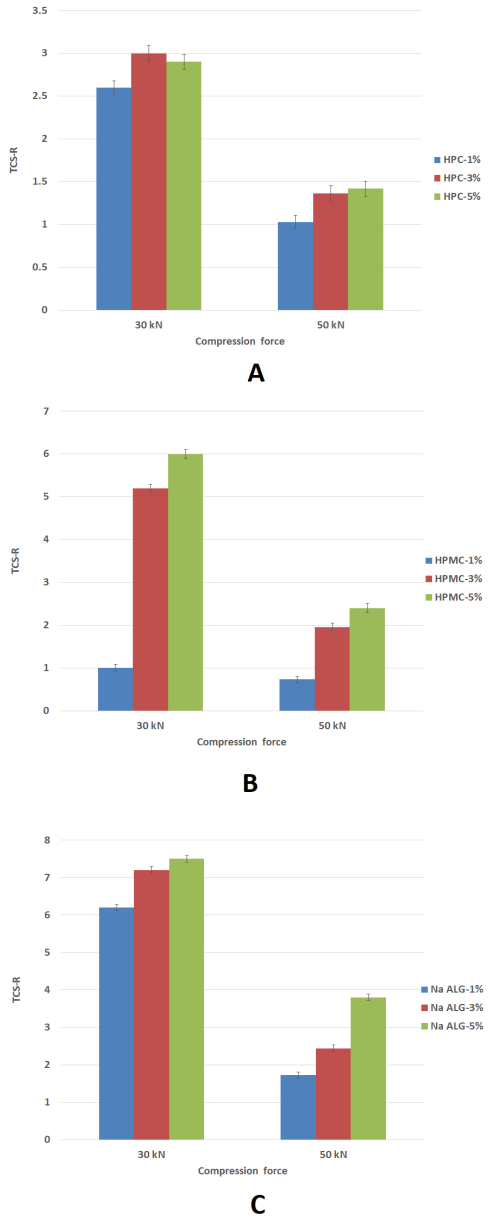

Figure 9 Relative tablet crushing strength (TCR-R) at 30 kN and 50 kN compression force and binder concentrations of 1, 3, and 5% for the three granulated systems.

started to occur at compression loads >300 kg for all the $CaCO_3$-binder samples (Figure 8).

TCS-R values of each $CaCO_3$-binder samples at the 1%, 3%, and 5% w/w binder concentrations are presented in Figure 9. Low and high compression forces of 30 and 50 kN were chosen to identify the force effect on the TCS-R values. These values of compression forces were chosen based on the large changes in tablet crushing strength above a compression force of 30 kN for all the $CaCO_3$-binder samples (Figure 9).

When the granulated and the reference (the un-granulated) $CaCO_3$ powders were compared (Figure 7), there were low and high regions of compression pressures which determined the observed wide and narrow differences, respectively in corresponding AUC values (Figures. 3-5) and tablet crushing strength values (Figure 7). Thus the AUC-R and TCS-R ratios were adopted to provide an indication of the extent of increase or decrease in the AUC and crushing strength values compared to the reference. These ratios potentially provide a more reliable indicator of the compression force and binder concentration required for the industrial processing of $CaCO_3$ than AUCs and tablet crushing strength absolute values.

For $CaCO_3$-HPC, data in Figure 8-A showed that a low compression load (300 kg) and an HPC concentration of 3% w/w could be used to increase the AUC-R to values greater than those that at high compression load (500 kg) and at 5% w/w binder. This suggests that the extent of deformation (brittle fracture) of $CaCO_3$-HPC granules is higher at low compression loads than at high compression loads. Interestingly, the AUC-R results are consistent with the TCS-R data in Figure 9-A for $CaCO_3$-HPC whereby high TCS-R values (2.6-3.0) occur at low compression force (30 kN- single punch) and 3% w/w binder. On the other hand, the low TCS-R values for $CaCO_3$-HPC (1.0-1.4) suggest that there is no added value in using a high compression force (50 kN) regardless of binder concentration.

For $CaCO_3$-HPMC, the higher binder concentration and lower compression loads presented higher AUC-R values, as shown in the data in Figure 8-B. The maximum AUC-R is attained at $CaCO_3$-5% w/w HPMC when compressed at 300 kg. This is consistent with the TCS-R results shown in Figure 9-B whereby $CaCO_3$-HPMC compressed at 30 kN displayed the highest TCS-R values at the 5% w/w binder. In fact, at all concentrations of the binder, $CaCO_3$-HPMC exhibited higher TCS-R values; 1-6 at 30 kN compared to 0.73-2.4 at 50 kN compression force.

The greatest crushing strength was obtained with the $CaCO_3$-Na-Alg granules at all compression forces (Figure 7). The data in Figure 8-C and 9-C show the effect of compression at low loads (300 kg) on AUC-R and TCS-R values, respectively. There was no difference in AUC-R values at binder concentrations of 1% and 3% w/w, which decreased at 5% (Figure 8-C). TCS-R results were consistent with AUC-R data, as decreasing the compression pressure resulted in higher TCS-R values. There were no significant differences in the TCS-R values (Figure 9-C), upon varying the binder concentration (6.2-7.2 at 300 kg). The highest TCS-R values were obtained for the $CaCO_3$-Na-Alg. This suggests that tablet properties of $CaCO_3$-Na-Alg were influenced more by the compression load than by the binder concentration.

Morphology

SEM testing of the granules was performed for visual confirmation of the granulation process. Granules were visualized at the maximum binder concentration used in this work, i.e., at the 5% w/w. SEM results for the reference sample are shown in Figure 10A, Figure 11A, and Figure 12A at different magnifications. The reference sample was not homogeneous in size as rock-shaped granules of planar and irregular surfaces were surrounded by tiny pieces of $CaCO_3$. The three granulated solutions produced a larger size and more regularly shaped particles than natural $CaCO_3$. This is clear when the particle shapes are viewed at 200x magnification (Figure 10B, C, D). When viewed at 2000x (Figure 11), the surface appeared to be made up of the same small particles of $CaCO_3$ for all the binders used. At 10000x magnification (Figure 12), some $CaCO_3$ crystals can be viewed on the surface in addition to small pieces, which are more likely to belong to the dried binder and/or $CaCO_3$ surrounding and covering the crystal particles. This observation applies to SEM results for HPC and HPMC binders in Figure 12. However, no $CaCO_3$ crystals were detected on the surface of $CaCO_3$ granulated with Na-Alg (Figure 12D).

The most desirable outcomes with respect to the AUC, P_k, and compact crushing strength were obtained with a binder concentration of 3%. It has been reported that there is a granule saturation level according to the binder content. Since the binder solution volume to

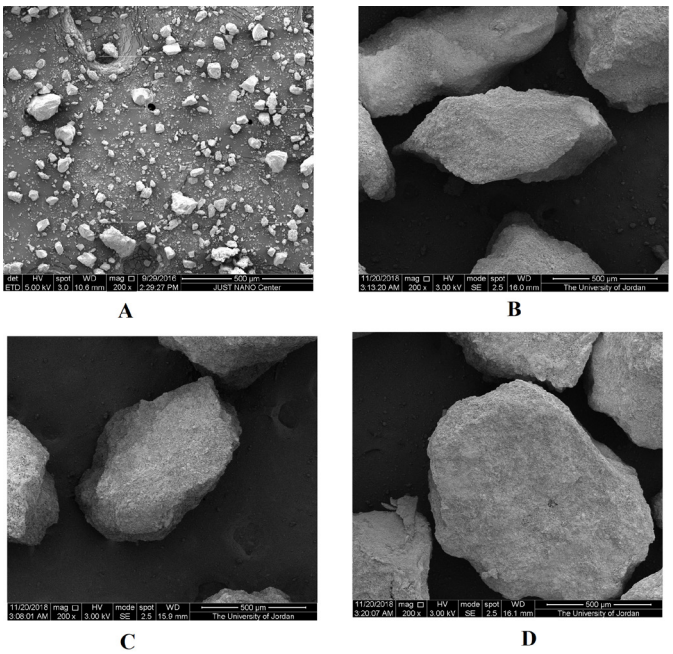

Figure 10 Particle shape and size of (A) natural $CaCO_3$, (B) with the binder HPC, (C) HPMC, (D) Na-Alg at 200x and particle size of 250-850 μm

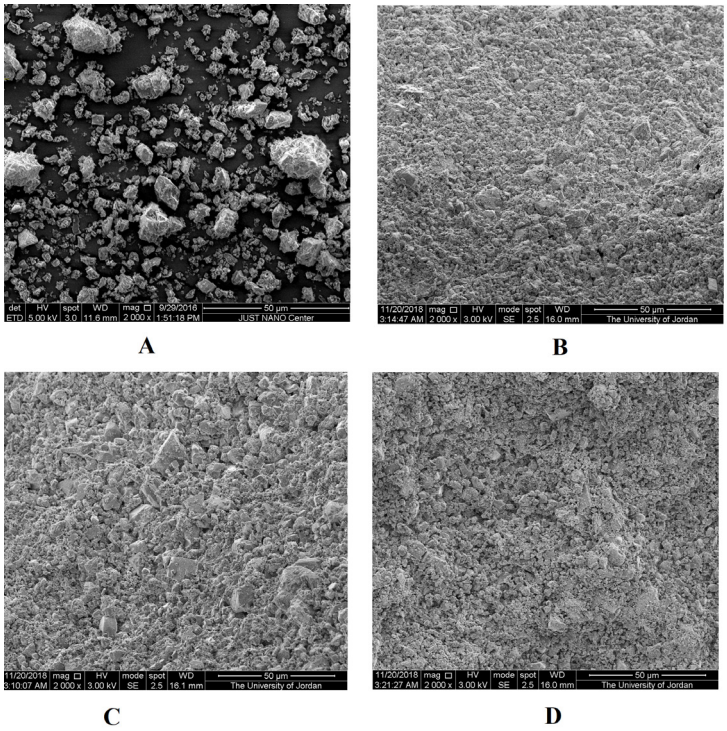

Figure 11 Particle shape and size of (A) natural $CaCO_3$, (B) with the binder HPC, (C) HPMC and (D) Na-Alg at 2000x and particle size of 250-850 μm

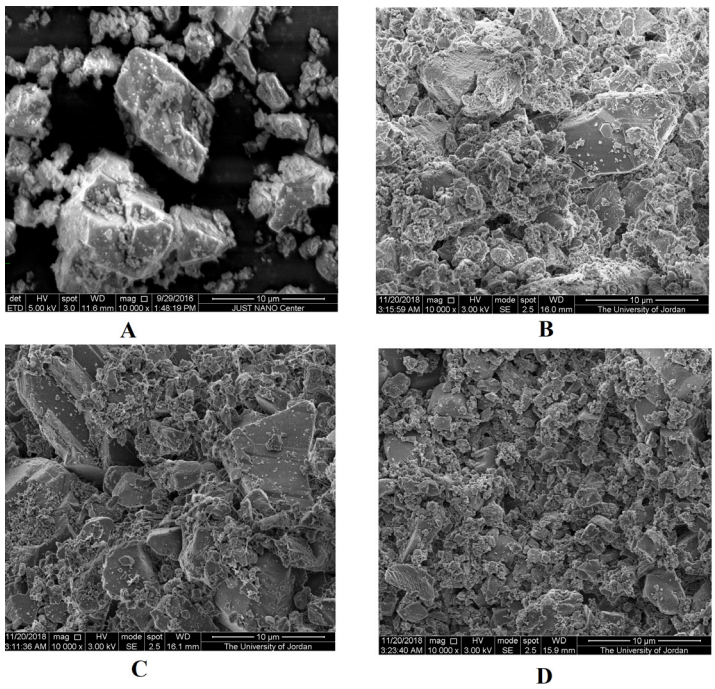

Figure 12 Particle shape and size of (A) natural $CaCO_3$, (B) with the binder HPC, (C) HPMC and (D) Na-Alg at 1000x and particle size of 250-850 μm.

$CaCO_3$ mass ratios were 25%, 46.4% and 63.2% for binder concentrations of 1%, 3%, and 5% respectively, this suggests that over saturation could be the case for the 5% w/w concentration of all the binders used in our work (33, 34). Binders are distributed at the periphery of the granules causing agglomeration of particles into lumps of individual particles. These lumps can be detected in the SEM micrographs (Figures 10-B, C, D at 200x magnification) resulting from the agglomeration of the individual $CaCO_3$ particles shown in Figure 10-A. The presence of particle agglomeration is obvious when granule surfaces are viewed at 2000x magnification (Figure 11). At 10,000x magnification, small individual particles of $CaCO_3$ appeared on the surface of the granules bound together by HPC and HPMC (Figure 12 B and C). It appeared that HPMC covered the $CaCO_3$ surface more uniformly than HPC. The absence of small particles on the surface of $CaCO_3$ granulated with Na-Alg (Figure 12D) may be related to the high viscosity of this binder. A high-water binding capacity may increase the volume of binder solution at which a change from granule growth to slurry or over-wetting occurs in the wet granulation. By not overshooting the granule growth regime, Na-Alg may be able to cause the greatest agglomeration of the largest number of different sized particles.

Table 4 Viscosity of binder solutions at 1, 3 and 5% (w/w) concentrations

BINDER	BINDER CONCENTRATION (%w/w)	VISCOSITY (mPa.s)*
HPC	1	46.19
	3	86.04
	5	199.53
HPMC	1	446.94
	3	762.18
	5	142.70
Na-Alg	1	294.66
	3	4141.90
	5	2929.50

*Shear rate was fixed at $0.01s^{-1}$

The viscosity of binder solutions

The aim of the viscosity studies was to link the behavior of powder compression with the solution properties of the binder. The viscosity of 1, 3, and 5% w/w of HPC, HPMC, and Na-Alg solutions were determined (Table 4). Viscosity of all binders increased from 1% w/w to 3% w/w. However, the viscosity was found to decrease for HPMC and Na-Alg, unlike HPC, at 5% w/w compared to the 3% w/w binder concentration.

Changes in the compression behavior due to changes in binder concentration were found to be correlated with changes in the viscosity of the granulating solution. HPMC and Na-Alg solutions reached maximum viscosities at 3% w/w, subsequently decreasing at 5% w/w binder concentration. These results are consistent with scientific and commercial data on Methocel™ and Na-Alg (35, 36). The decrease at the 5% w/w binder concentration is attributed to intra-chain electrostatic repulsion of charges on the backbone of the polymeric molecules (37). It has to be emphasized that the measured viscosities in the reported data (38) do not involve the measurement of torque change with an increase in spindle speed (or shear rate). Otherwise, measured viscosities of Na-Alg and HPMC through shear stress/shear rate relation would generally indicate a decrease in viscosity with concentration (39, 40). It is suggested that such a decrease, which reflects the shear-thinning phenomenon upon increasing the shear rate, does not correlate to the actual viscosities for granulation. Nevertheless, the maximum viscosities of Na-Alg and HPMC at 3% w/w correlated with the observed high granule strength. The viscosity of HPC was lesser, as was its granule strength when compared to Na-Alg and HPMC (Table 4).

Specific surface area (SSA) of $CaCO_3$-binder granules

Generally, wet granulation results in a decrease in specific surface area. In this study, the increase in binder concentration from 1-5% for $CaCO_3$ resulted in values of SSAs shown in Table 5. Wet granulation increased the particle size of the raw $CaCO_3$ from 30-120 μm to 250-850 μm. The granules produced were composed of several $CaCO_3$ particles adhered together by the

binder.

Theoretically, the minimum decrease in SA based on a spherical particle when its size undergoes an increase can be estimated as shown in Equations 3 and 4:

$$SA = 4\pi r^2 \quad \text{Eq. 3}$$

$$V = \frac{4}{3}\pi r^3 \quad \text{Eq. 4}$$

where; SA and V are the surface area and volume of a sphere, respectively.

The mass (m) of a sphere is shown in Equation 5:

$$m = \rho V = \frac{4}{3}\pi r^3 \rho \quad \text{Eq. 5}$$

Where; ϱ is the density.

Accordingly, the SSA is obtained using Equation 6:

$$SSA = \frac{SA}{m} = \frac{4\pi r^2}{\frac{4}{3}\pi r^3 \rho} = \frac{3}{\rho r} \quad \text{Eq. 6}$$

The change in the ratio of the SSA when the particle size undergoes an increase from r_1 to r_2 is shown in Equation 7:

$$\frac{SSA_2}{SSA_1} = \frac{\frac{3}{\rho r_2}}{\frac{3}{\rho r_1}} = \frac{r_1}{r_2} \quad \text{Eq. 7}$$

Table 5 shows that SSA decreases at 1-3% binder concentration for all binders followed by an increase at 3-5% for HPC and HPMC, but a continued decrease for Na-Alg. Theoretically, an increase in particle size results in a decrease in its SSA. SEM indicates that $CaCO_3$ particles agglomerate to an approximate particle size

Table 5 Specific surface area values of raw and granulated $CaCO_3$ at different binder concentration (% w/w)

SYSTEM	BINDER CONCENTRATION (%, w/w)	SSA (m^2/g)
$CaCO_3$	0	1.801
$CaCO_3$-HPC	1	2.007
	3	0.888
	5	1.389
$CaCO_3$- HPMC	1	1.527
	3	1.009
	5	1.539
$CaCO_3$-Na-Alg	1	2.656
	3	2.56
	5	2.018

of 500 micrometers (Figure 10) from a native size of 120 μm, an SSA ratio of ~4. However, the SSA ratios at 3% and 1% binder concentrations for HPC, HPMC, and Na Alg are 2.3, 1.5, and 1.0 respectively (Table 5). It is speculated that this significantly lower change in the SSA could be attributed to the mechanism of binding and surface structure of $CaCO_3$ particles, where the agglomerated porosity of the granule is sufficiently large to partly negate the increased particle size. Therefore, the measured SSA does not indicate a size enlargement of the same particle but instead a new surface structure comprising numerous $CaCO_3$ particles adjacent to each other due to binding. This can be seen from the SEM photographs in Figure 10 (B, C, D). However, SSA values increased at a binder concentration of 5% w/w for HPC and HPMC. It is speculated that at a significantly greater granulating volume to $CaCO_3$ mass ratio of 63.2% v/w, the granulation approaches the slurry stage, with consequent partial granule de-agglomeration causing an increase in SSA. On the other hand, the SSA continued to decrease upon increasing the Na-Alg concentration from 3% to 5% w/w and thus may indicate that this binder may not have reached the slurry stage even at a granulation volume to $CaCO_3$ mass ratio of 63.2%. Interestingly, the viscosity of 3% and 5% Na-Alg solutions are an order of magnitude greater than those of the HPC and HPMC solutions of similar concentrations. This greater water-binding capacity may be partly responsible for the transition of the wet granulation from the granule growth stage

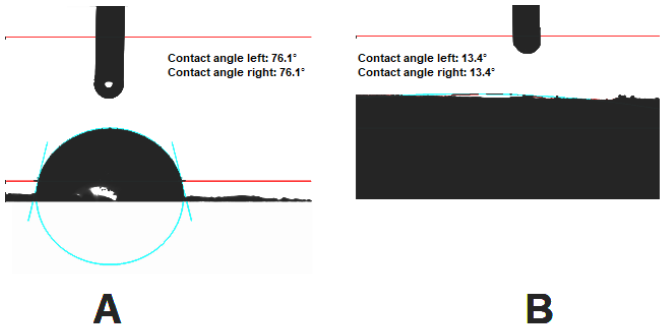

Figure 13 Contact angle of droplet of binder solution on the surface of $CaCO_3$ compacts, (A) Na-Alg., (B) HPC or HPMC.

to the slurry or over-wetting stage at a higher binder solution volume to $CaCO_3$ mass ratio.

The specific surface area (SSA) of granules correlates with the extent of wet granulation taking place for the agglomeration of particles. Theoretically, upon increasing the volume of binding solution, wet granulation delivers a maximum limit of wet mass cohesiveness above which the granulated powder system changes from a thick paste into a slurry (40-42). Consequently, the initial decrease in SSA for HPC, HPMC, and Na-Alg (when their concentrations were increased from 1 to 3%) may be a direct indication of increased agglomeration of the $CaCO_3$ granules.

Contact angle measurements

At all binder concentrations, (1-5% w/w), Na-Alg formed intact droplets. A representative image of such a droplet for all concentrations is shown in Figure 13A at a binder concentration of 5% w/w. On the other hand, HPC and HPMC droplets in the same concentration range (1-5% w/w) penetrated the compacts (Figure 13 B).

Contact angle values of binders are related to their extent of wettability on the surface of $CaCO_3$. Such measurements are important to determine; especially when the SSA of $CaCO_3$-Na-Alg granules decreased at a binder concentration of 5% w/w. Such a decrease suggests that the binder is still effective in decreasing the intra-granular porosity of the granules at this concentration value (5% w/w). This can be justified by the low wetting ability of Na-Alg to cover the $CaCO_3$ surface upon granulation. Such low wettability was indicated by the high contact angle made by a Na-Alg droplet (5% w/w) on the surface of a $CaCO_3$ compact (Figure 13 A). In contrast, as stated previously, HPC and HPMC droplets (5% w/w) penetrated inside the $CaCO_3$ surface as no intact droplets were formed (Figure 13 B). It can be argued that the high values for crushing strength of the compacts in the binder type order; Na-Alg>HPMC>HPC and in the binder concentration order; 5%>3%>1%, is due to the high viscosity of the binder solution at the same binder type and concentration. This was very clear when the contact angle is used. The lower viscosity of HPC and HPMC solutions compared with that of the Na-Alg solution allows them to penetrate the porous surface of $CaCO_3$, hence a greater amount is required to form similar-sized agglomerates. Due to the high viscosity of Na-Alg and its ability to gel, the alginate forms a gel at the $CaCO_3$ surface, hence including more $CaCO_3$ native particles in an agglomerate, for a given amount of binder. This can be attributed to a dual effect; the film-forming property of the Na-Alg and its gelling at the surface of $CaCO_3$ particles. It is also known that Ca^{+2} ions in the presence of Na-Alg form a cross-linked matrix (43).

Formulation and physical stability of $CaCO_3$ tablets

Crushing force and disintegration time were measured during the storage of physical compacts. Physical stability analysis performed on $CaCO_3$ preparations is presented in Tables 6 and 7 for the tablets comprising HPMC and Na-Alg respectively. Tablet hardness decreased and disintegration time and friability increased during storage. Nevertheless, tablet properties were within compendial specifications after 6 months of storage at 40°C/closed conditions. At 40°C, 75% RH, there was an increase in tablet hardness, probably due to increased binding of granules further strengthening the compacts. Calcium carbonate tablets were able to maintain their most important physical properties, i.e., crushing force and disintegration within predesigned limits during storage.

Table 6 Physical stability results for $CaCO_3$ tablets prepared with HPMC binder and stored at 40 °C, 75% RH for 6 months

DURATION	STORAGE CONDITION	TABLET HARDNESS (N) (NOT LESS THAN 100 N)	TABLET DISINTEGRATION TIME (LESS THAN 15 MIN)	FRIABILITY (%) (NOT MORE THAN 1%)	WATER CONTENT (%) (NOT MORE THAN 1.5%)
Initial	Initial	205-246, SD=9.1	30 s -45 s	0.27	0.36
3rd month	40 °C, 75% RH	238-267, SD=3.5	1 min-2 min	0.15	0.99
	RT	186-223, SD=8.2	50 s-1.10 min	0.46	0.45
6th month	40 °C, 75% RH	259-304, SD=5.5	4 min -5 min	0.29	1.20
	RT	167-194, SD=6.7	45 s – 66 s	0.38	0.47

Table 7 Physical stability results for $CaCO_3$ tablets prepared with Na-alg. binder and stored at 40°C, 75% RH for 6 months.

DURATION	STORAGE CONDITION	TABLET HARDNESS (N) (NOT LESS THAN 100 N)	TABLET DISINTEGRATION TIME (LESS THAN 15 MIN)	FRIABILITY (%) (NOT MORE THAN 1%)	WATER CONTENT (%) (NOT MORE THAN 1.5%)
Initial	Initial	259-286, SD=6.8	40 s -62 s	0.19	0.42
3rd month	40°C, 75% RH	273-293, SD=10.5	5 min-7 min	0.15	1.19
	RT	216-241, SD=9.1	1.0 min-1.30 min	0.39	0.44
6th month	40°C, 75% RH	286-318, SD=9.4	9 min -12 min	0.11	1.38
	RT	189-215, SD=7.8	1.5 min – 2.0 min	0.39	0.43

CONCLUSIONS

Granules ready for compression containing $CaCO_3$ from natural sources were produced at an optimum binder concentration of 3% w/w for the granulating agents tested namely HPC, HPMC, and Na-Alg. The optimum binder concentration was determined from measurements of the area under the compression curve (AUC) and P_K values associated with the load-displacement curve and Kawakita analysis, respectively. This study further demonstrated that when granulated powders are compressed and compared with the natural $CaCO_3$ powders, relatively lower compression loads have a disproportionately greater effect in increasing powder compression (AUC-R) and tablet properties (TCS-R) than relatively higher compression loads. The resultant optimum concentration of the binders used was attributed to viscosity and specific surface area variations, which both reached optimum values at the 3% w/w binder concentration. Finally, the ready for compression granules of natural origin $CaCO_3$ comprising 3% binder, can be used as a directly compressible powder. This granulated powder demonstrated its ability to form compacts that retained their physical properties when stored at 40°C, 75% RH for 6 months.

FUNDING

This research received no external funding.

CONFLICT OF INTEREST

The authors declare no conflict of interest. The Jordanian Pharmaceutical Manufacturing Company (JPM) did not have any role in the design of the study; in the collection, analyses, or interpretation of data; in the writing of the manuscript; or in the decision to publish the results.

ACKNOWLEDGMENTS

The authors would like to thank the University of Jordan and the University of Greenwich for their ongoing support. The authors also wish to thank the Jordanian Pharmaceutical Manufacturing Co. (JPM) for providing materials, laboratory, and testing facilities. The authors would like to thank Mr. Akram Bikdash

for his help in carrying out some of the granulation experiments.

REFERENCES

1 Al Omari MM, Rashid RI, Qinna NA, Jaber AM, Badwan AA. Calcium Carbonate. Profiles Drug. Subst. Excip. Relat Methodol. 41: 31-132, 2016.

2 Montes-Hernandez G, Renard F, Geoffroy N, Charle L, Pironon J. Calcite precipitation from CO2–H2O–Ca(OH)2 slurry under high pressure of CO_2. J. Cryst. Growth. 308: 228–236, 2007.

3 Tang H, Yu J, Zhao X, Ng HLD. Creation of calcite hollow microspheres with attached bundles of aragonite needles. Cryst. Res. Technol. 43: 473–478, 2008.

4 United States Pharmacopeia Convention, United States Pharmacopeia 38/National Formulary 33 (USP 38/NF 33), Description and Solubility, Vol. 1, USP Convention Inc., Maryland, 2015.

5 Murakami FS, Rodrigues PO, de Campos CMT, Silva MAS. Physicochemical study of $CaCO_3$ from egg shells. Cieˆnc. Tecnol. Aliment. Campinas. 27: 658–662, 2007.

6 Hanzlik RP, Fowler SC, Fisher DH. Relative Bioavailability of Calcium from Calcium Formate, Calcium Citrate, and Calcium Carbonate. J Pharmacol Exp Ther. 313: 1217-1222, 2005.

7 Straub DA. Calcium Supplementation in Clinical Practice: A Review of Forms, Doses, and Indications. Nutr Clin Pract. 22: 286-296, 2007.

8 Tovey GD. Pharmaceutical Formulation: The Science and Technology of Dosage Forms, first ed., Royal Society of Chemistry, Cambridge, UK, 2018.

9 Costa LMM, Olyveira GM, Salomão R. Precipitated calcium carbonate nano-microparticles: applications in drug delivery, Adv Tissue Eng Regen Med Open Access. 3: 336–340, 2017.

10 Kim DS, Lee CK. Surface modification of precipitated calcium carbonate using aqueous fluosilicic acid. Appl. Surf. Sci. 202: 15–23, 2002.

11 Levin R, Lang K, Murphy G, Dibble J. calcium carbonate granulation, United States Patent. US20070178154A1, 2007.

12 Markl D, Wang P, Ridgway C, Karttunen AP, Chakraborty M, Bawuah P, Pääkkönen P, Gane P, Ketolainen J, Peiponen KE, Zeitler JA. Characterization of the Pore Structure of Functionalized Calcium Carbonate Tablets by Terahertz Time-Domain Spectroscopy and X-Ray Computed Microtomography. Journal of Pharmaceutical Sciences. 106: 1586-1595, 2017.

13 Santoso A, Handoko A, Hak-Kim C, Warren HF, Zhenbo T, Runyu Y, Aibing Y. Agglomerate strength and dispersion of pharmaceutical powders. Journal of Aerosol Science. 42: 285–294, 2011.

14 Zhang J, Guo J, Li T, Li X. Chemical Surface Modification of Calcium Carbonate Particles by Maleic Anhydride Grafting Polyethylene Wax. International Journal of Green Nanotechnology: Physics and Chemistry. 1: 65-71, 2010.

15 Preisig D, Haid D, Varum FJO, Bravo R, Alles R, Huwyler J, Puchkov M. Drug Loading into Porous Calcium Carbonate Microparticles by Solvent Evaporation. Eur. J. Pharm. Biopharm. 87: 548–558, 2014.

16 Stirnimann T, Atria S, Schoelkopf J, Gane PAC, Alles R, Huwyler J, Puchkov M. Compaction of functionalized calcium carbonate, a porous and crystalline microparticulate material with a lamellar surface, International Journal of Pharmaceutics. 466: 266–275, 2014.

17 Withiam MC, Mehra DK, Cornelius JM. Rapidly disintegrating low friability tablets comprising calcium carbonate. US Patent. US 2007/0196474 A1, 2007.

18 Olsen PM, Bertelsen PE, Thisted T, Aage HR. Improved dissolution stability of calcium carbonate tablets, EP 2358374 A1, 2011.

19 Lang KW, Dibble JW, Levin R, Murphy GB. Calcium carbonate granulation, US 7807125 B2, 2010.

20 Bacher C, Olsen PM, Bertelsen P, Kristensen J, Sonnergaard JM. Improving the compaction properties of roller compacted calcium carbonate, International Journal of Pharmaceutics. 342: 115–123, 2007.

21 Gerard DE, Schoelkopf J, Gane PAC, Stirnimann T, Alles R, Puchkov M, Huwyler J. Fast disintegrating solid dosage form formulation comprising functionalized calcium carbonate and method of their manufacture, EP2916816A1, 2015.

22 Lang KW, Levin R, Dibble JW, Murphy GB. Calcium carbonate granulation, US 7198653, 2007.

23 Flores LE, R.L. Arello, Esquivel JJ. Study of load capacity of avicel PH-200 and cellactose, two direct-compression excipients, using experimental design. Drug Dev Ind Pharm. 26: 465-69, 2000.

24 Schmidt PC, Rubensdorfer CJ. Evaluation of ludipress as a multipurpose excipients for direct compression part I: Powder characteristics and tableting properties. Drug Dev Ind Pharm. 20: 2927-2952, 1994.

25 Chaheen M, Bataille B, Yassine A, Belamie E, Sharkawi T. Development of Coprocessed Chitin-Calcium Carbonate as Multifunctional Tablet Excipient for Direct Compression, Part 2: Tableting Properties, Journal of Pharmaceutical Sciences. 108: 3319-3328, 2019.

26 Gabbott I, Chouk V, Pitt MJ, Gorham DA, Salman AD. Chapter 27 Descriptive Classification: Failure Modes of Particles by Compression, in: A. Salman, M. Ghadiri, M. Hounslow (Eds.), Handbook of Powder Technology, Elsevier, 2009; pp. 1121-1147.

27 Pusapati RT, Kumar MVRK, Rapeti SS, Murthy TEGK. Development of co-processed excipients in the design and evaluation of atorvastatin calcium tablets by direct compression method. International Journal of Pharmaceutical

Investigation. 4: 102-106, 2014.

28 Bezerra MA, Santelli RE, Oliveira EP, Villar LS, Escaleira LA. Response surface methodology (RSM) as a tool for optimization in analytical chemistry. Talanta. 76: 965-977, 2008.

29 Nordstrom J, Klevan I, Alderborn G. A particle rearrangement index based on the Kawakita powder compression equation, J. Pharm. Sci. 98: 1053–1063, 2009.

30 Patel S, Kaushal AM, Bansal AK. Compression physics in the formulation development of tablets. Crit Rev Ther Drug Carrier Syst. 23: 1-65, 2006.

31 Brunauer S, Emmet PH, Teller E. Adsorption of gases in multimolecular layers. J Am Chem Soc. 60: 309–319, 1938.

32 Badwan AA, Rashid I, Al Omari MMH, Darras FH. Chitin and Chitosan as Direct Compression Excipients in Pharmaceutical Applications, Mar Drug. 19: 1519-1547, 2015.

33 Newitt DM, Conway JJM. A contribution to the theory and practice of granulation. Trans. I. Chem. Eng. 36: 422-441, 1958.

34 Heim A, Gluba T, Obraniak A, Gawot-Mlynarczyk E, Blaszczyk M. The effect of wetting parameters on mechanical strength of granulated material. Physicochemical Problems of Mineral Processing. 40: 237-245, 2006.

35 Lima AMF, Soldi V, Borsali R. Dynamic light scattering and viscosimetry of aqueous solutions of pectin, sodium alginate and their mixtures: effects of added salt, concentration, counterions, temperature and chelating agent. J. Braz. Chem. Soc. 20: 1705-1714, 2009.

36 Dow Pharma & Food Solutions Corporate Profile. How to Prepare Aqueous Solutions of METHOCEL™ Cellullose Ethers. METHOCEL™ - Technical Bulletin, 10-2013.

37 Zhonga D, Huanga X, Yanga H, Cheng R. New insights into viscosity abnormality of sodium alginate aqueous solution. Carbohydrate Polymers. 81: 948–952, 2010.

38 Brzezińska M, Szparaga G. The effect of sodium alginate concentration on the rheological parameters of spinning solutions, Autex Research Journal. 15: 123-126, 2015.

39 Belalia F, Djelali N. Rheological Properties of Sodium Alginate Solutions. Rev. Roum. Chim. 59: 135-145, 2014.

40 Fatimi A, Tassin JF, Quillard S, Axelos MA, Weiss P. The rheological properties of silated hydroxylpropylmethylcellulose tissue engineering matrices. Biomaterials. 29: 533-543, 2008.

41 Rowe RC, Sadeghnejad GR. The rheology of microcrystalline cellulose powder / water mixes - measurement using a mixer torque rheometer. Int. J. Pharm. 41: 231-236, 1987.

42 Hancock BC, York P, Rowe RC, Parker MD. Characterisation of wet masses using a mixer torque rheometer: 1. Effect of instrument geometry. Int. J. Pharm. 76: 239-245, 1991.

43 Al-Mousa S, Abu Fara D, Badwan AA. Evaluation of Parameters involved in the Preparation and Release of Drug Loaded in Cross-linked Matrices of Alginate. Journal of Controlled Release. 57: 223-232, 1999.